Dalton Transactions

PAPER

View Article Online
View Journal | View Issue

Cite this: *Dalton Trans.*, 2017, **46**, 15710

Synthesis of 13-vertex dimetallacarboranes by electrophilic insertion into 12-vertex ruthenacarboranes†

Dmitry S. Perekalin, *[a] Konstantin A. Lyssenko, [a] Alexander R. Kudinov,‡[a] Maddalena Corsini[b] and Fabrizia Fabrizi de Biani [b]

Received 18th September 2017,
Accepted 13th October 2017

DOI: 10.1039/c7dt03504g

rsc.li/dalton

The electrophilic insertion of organometallic species into metallacarboranes was studied in detail for the model compound – the 12-vertex *closo*-ruthenacarborane anion $[Cp^*Ru(C_2B_9H_{11})]^-$ (**1**). Reactions of the anion **1** with the 12-electron cationic species $[M(ring)]^+$ (M(ring) = RuCp, RuCp* and $Co(C_4Me_4)$) gave the 13-vertex *closo*-dimetallacarboranes $Cp^*Ru(C_2B_9H_{11})M(ring)$. Similar reactions of the neutral ruthenacarborane $Cp^*Ru(Me_2S\text{-}C_2B_9H_{10})$ produce the cationic dimetallacarboranes $[Cp^*Ru(Me_2S\text{-}C_2B_9H_{10})M(ring)]^+$. The symmetrical 13-vertex diruthenacarboranes $(C_5R_5)Ru(R_2C_2B_9H_9)Ru(C_5R_5)$ can be prepared by the direct reactions of $Tl_2[7,8\text{-}R_2\text{-}7,8\text{-}C_2B_9H_9]$ (R = H and Me) with two equivalents of $[CpRu(MeCN)_3]^+$ or $[Cp^*RuCl]_4$. The insertions of the 14-electron cationic species $[M(ring)]^+$ (M(ring) = NiCp, NiCp* and $Co(C_6Me_6)$) into **1** gave the 13-vertex dimetallacarboranes $Cp^*Ru(C_2B_9H_{11})M(ring)$, which have a distorted framework with one open face. The structures of $Cp^*Ru(C_2B_9H_{11})Co(C_4Me_4)$ and $Cp^*Ru(C_2B_9H_{11})NiCp$ were established by X-ray diffraction. Some of the 13-vertex dimetallacarboranes have two electrons less than required by Wade's rules. This violation is explained by the absence of the appropriate pathway for the distortion of the framework.

Introduction

Carboranes and metallacarboranes represent a unique class of cluster molecules with high thermal and chemical stability and unusual reactivity.[1] These properties make them useful building blocks for non-coordinating anions,[2] dendrimers,[3] functional materials,[4] and catalysts.[5] In recent years a significant progress has been made in the field of supericosahedral species, which have more than 12 vertices in the cage.[6,7] The synthesis of such compounds is usually based on the reduction of *closo*-clusters to *nido*-dianions and subsequent addition of a new vertex (boron or metal).[8] An attractive alternative approach, namely, the direct insertion of metal complexes into *closo*-clusters, has been long known only for small (sub-icosahedral) frameworks.[9] Recently, it has been found that the electrophilic insertion of cationic species $[M(ring)]^+$ is an effective method for the synthesis of supericosahedral metallacarboranes.[6a–c,10] Herein we report the detailed investigation of this reaction for the model 12-vertex ruthenacarborane anion $[Cp^*Ru(C_2B_9H_{11})]^-$ (**1**). The unusual 13-vertex dimetallacarboranes obtained in this way were studied by theoretical and physicochemical methods.

Results and discussion

Insertion of 12-electron $[M(ring)]^+$ species

We studied the reaction of ruthenacarborane anion **1** with $[(C_5R_5)Ru(MeCN)_3]^+$ (R = H and Me) (Scheme 1). It was

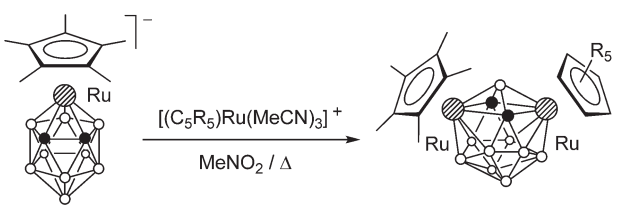

1 R = H (**2a**), Me (**2b**)

Scheme 1

[a]*A. N. Nesmeyanov Institute of Organoelement Compounds, Russian Academy of Sciences, 119991 Moscow, Russian Federation. E-mail: dsp@ineos.ac.ru*
[b]*INSTM and Dipartimento di Biotecnologie, Chimica e Farmacia dell'Università di Siena, Via Aldo Moro, 53100 Siena, Italy*

†Electronic supplementary information (ESI) available: Experimental synthetic procedures, crystallographic data files for the structures of **5** and **9a**, the results of DFT calculation (optimized geometries, frequencies, and energy data). CCDC 1570483 and 1570484. For ESI and crystallographic data in CIF or other electronic format see DOI: 10.1039/c7dt03504g

‡Deceased.

expected that electrophilic attack of the species $[Ru(C_5R_5)]^+$ would proceed at the Cp* ring to give the triple-decker complex $(C_5R_5)Ru(\mu\text{-}Cp^*)Ru(C_2B_9H_{11})$, similar to the formation of $[(C_5R_5)Ru(\mu\text{-}Cp^*)RuCp^*]^+$ by the reaction of the same fragments with Cp^*_2Ru.[11] However, an electrophilic insertion into the ruthenacarborane cage occurred instead giving the 13-vertex diruthenacarboranes **2a**,**b** in *ca.* 50% yield.[10]

The precursor anion **1** was obtained in 72% yield by the reaction of thallium dicarbollide $Tl_2[7,8\text{-}C_2B_9H_{11}]$ with $[Cp^*RuCl]_4$ in acetonitrile (Scheme 2); the formation of **2b** was not detected in this case. In contrast, if this reaction was carried out in THF, complex **1** reacted further with the second equivalent of $[Cp^*RuCl]_4$ giving **2b** even at −78 °C. This can be explained by the higher reactivity of the intermediate solvate species $[Cp^*Ru(THF)_3]^+$ over $[Cp^*Ru(MeCN)_3]^+$ due to the lower coordinating ability of THF. Accordingly, complex **2b** can be easily prepared by the direct reaction of $Tl_2[7,8\text{-}C_2B_9H_{11}]$ with two equivalents of $[Cp^*RuCl]_4$. The analogous reaction of $Tl_2[7,8\text{-}C_2B_9H_{11}]$ with two equivalents of $[CpRu(MeCN)_3]^+$ gave the parent compound **2c**, while the reaction of the dimethyl-substituted derivative $Tl_2[7,8\text{-}Me_2\text{-}7,8\text{-}C_2B_9H_9]$ with $[Cp^*RuCl]_4$ produced the methylated complex **2d** (Scheme 3).

As a result of the insertion the cage carbon atoms become separated by one boron atom. We suggested that the presence of a small bridge between the carbons would prohibit this process. Indeed, no insertion takes place in the case of the ruthenacarborane anion **3** having the CH_2OCH_2 bridge (Scheme 4). The oxidative substitution product **4** was formed instead if the reaction is carried out in THF.[12] A similar reaction in non-coordinating solvents such as CH_2Cl_2 results in a complex mixture of products.

The reaction of **1** with the $[Co(C_4Me_4)]^+$ fragment (in the form of labile complexes $[(C_4Me_4)Co(MeCN)_3]^+$ or $[(C_4Me_4)Co(C_6H_6)]^+$)[13] gives the 13-vertex cobaltaruthenacarborane **5** in *ca.* 50% yield (Scheme 5). The competitive reaction of **1** with an equimolar mixture of the acetonitrile complexes $[(C_4Me_4)Co(MeCN)_3]^+$ and $[Cp^*Ru(MeCN)_3]^+$ in THF produces compounds **5** and **2b** in a 3 : 1 ratio. The faster insertion of the cobalt fragment can be attributed to the higher lability of the acetonitrile ligands in $[(C_4Me_4)Co(MeCN)_3]^+$.

The neutral ruthenacarborane 3-Cp*-4-SMe_2-3,1,2-$RuC_2B_9H_{10}$ (**6**) with the charge-compensating substituent SMe_2 is also capable of undergoing the insertion of the $[M(ring)]^+$ species. Thus, the reaction of **6** with $[(C_5R_5)Ru(MeCN)_3]^+$ (R = H and Me) or $[(C_4Me_4)Co(MeCN)_3]^+$ in refluxing nitromethane gives dimetallacarboranes **7a**,**b** and **8** (Scheme 6).[14]

The $^{11}B\{^1H\}$ NMR spectra of the dimetallacarboranes obtained display the sharp singlet at about 100 ppm corresponding to the bridging boron atom, having the lowest coordination number.[15] The signals of the other boron atoms lie in the −10 to 40 ppm range. The ^1H NMR spectra show high-field signals corresponding to CH vertexes at about −1 ppm. We suggest that these spectral anomalies are caused by the unusual electronic structure of the compounds (*vide infra*).

The structures of **2b**,[10] **5**, and **7b**$[Co(C_2B_9H_{11})_2]$[16] were established by X-ray diffraction. Compound **5** possesses the expected 13-vertex *closo*-dimetallacarborane (Fig. 1). The distances from the Ru and Co atoms to the bridging boron atom

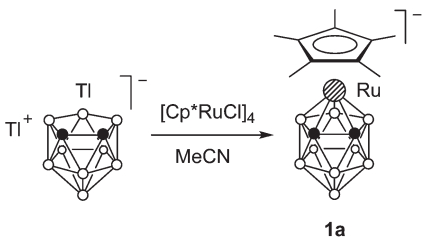

1a

Scheme 2

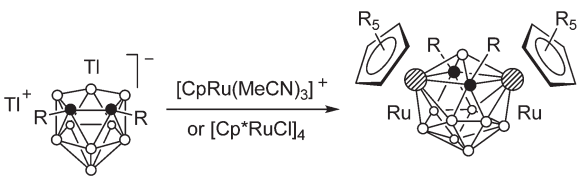

R = H (**2c**), Me (**2d**)

Scheme 3

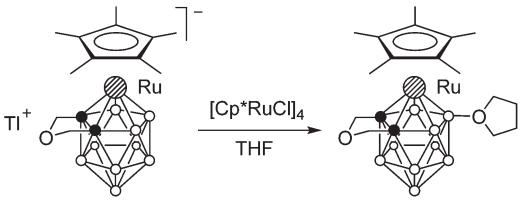

3 **4**

Scheme 4

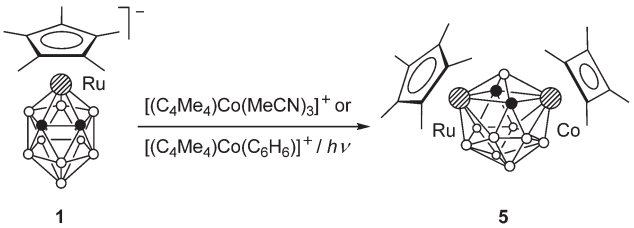

1 **5**

Scheme 5

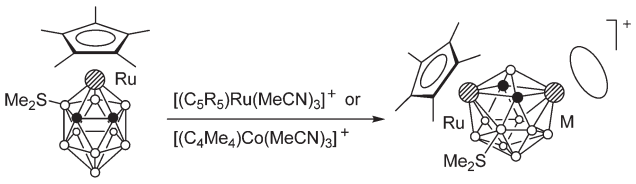

6 M(ring) = RuCp (**7a**), RuCp* (**7b**), $Co(C_4Me_4)$ (**8**)

Scheme 6

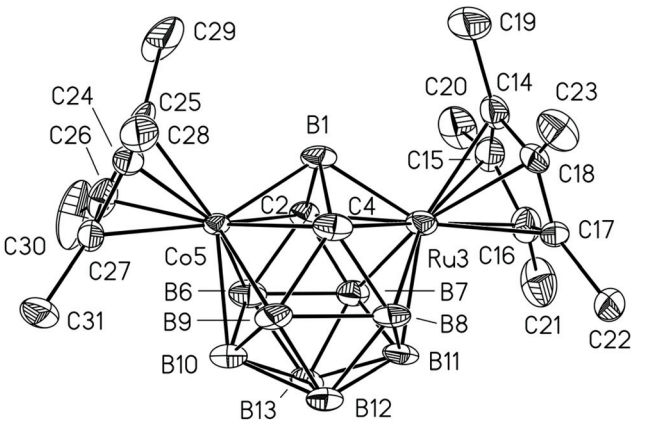

Fig. 1 The molecular structure of **5** in 50% thermal ellipsoids. The hydrogen atoms are omitted for clarity. Selected interatomic distances (Å): Ru3–C2 2.193(5), Ru3–C4 2.195(5), Ru3–B1 2.050(6), Ru3–B7 2.194(6), Ru3–B8 2.176(6), Ru3–B11 2.201(6), Co5–C2 2.120(5), Co5–C4 2.136(5), Co5–B1 1.985(6), Co5–B6 2.112(6), Co5–B9 2.121(6), Co5–B10 2.165(6), B1–C2 1.689(8), B1–C4 1.677(7), Ru3···Cp* 1.852, Co5···C_4Me_4 1.777, Ru3···Co5 3.4042(7).

B1 (Ru3–B1 2.050, Co5–B1 1.985 Å) are much shorter than other M–B distances (av. Ru3–B 2.192, Co5–B 2.136 Å). The long Ru3···Co5 distance (3.404 Å) suggests that there is no direct interaction between metal atoms.

Despite the facile synthesis of **2a–d** and **5**, the reactions of **1** with many other 12-electron half-sandwich complexes do not give the insertion products. Thus, treatment of the anion **1** with $[FeCp]^+$, $[Mn(CO)_3]^+$, $[Rh(cod)]^+$, $[Ir(cod)]^+$, $[CoCp]^{2+}$, $[RhCp^*]^{2+}$, and $[Ru(C_6H_6)]^{2+}$ species in the form of their labile complexes leads only to decomposition products (most probably *via* the oxidation of anion **1**). The variety of 12-vertex metallacarboranes capable of undergoing insertion reaction is also limited. The ferracarborane anion $[CpFe^{II}C_2B_9H_{11}]^-$ (iron analog of **1**) is oxidized by $[Cp^*RuCl]_4$ to give $CpFe^{III}C_2B_9H_{11}$. On the other hand, compounds $CpCo^{III}C_2B_9H_{11}$ and $CpRh^{III}C_2B_9H_{11}$ do not react with the $[RuCp^*]^+$ species.

Insertion of 14-electron $[M(ring)]^+$ species

The dimetallacarboranes **2a–d**, **5**, **7a,b**, and **8**, obtained by the insertion of 12-electron species $[Ru(C_5R_5)]^+$ and $[Co(C_4Me_4)]^+$, have two electrons less than required by Wade's rules (*vide infra*). In order to obtain dimetallacarboranes that obey Wade's rules, we studied the insertion of 14-electron species $[Ni(C_5R_5)]^+$ and $[Co(C_6Me_6)]^+$ into **1**. It was found that the reaction of **1** with $[CpNi(SMe_2)_2]^+$ or $[Cp^*NiCl]_2$ gives the 13-vertex nickela-ruthenacarboranes **9a,b** (Scheme 7). A similar reaction with $[(C_6Me_6)_2Co]^+$ gives cobalta-ruthenacarborane **10**.

Despite the formal similarity of the reactions with 12- and 14-electron cationic species, the structures of **9a,b** and **10** are notably different from those of **2a,b** and **5**. The X-ray diffraction study reveals that the framework of **9a** is strongly distorted from the expected C_s symmetry (Fig. 2; overlay of the structures of **5** and **9a** is shown in the ESI†). The key feature of this structure is the significant non-equivalence of Ni–C_{cage} distances

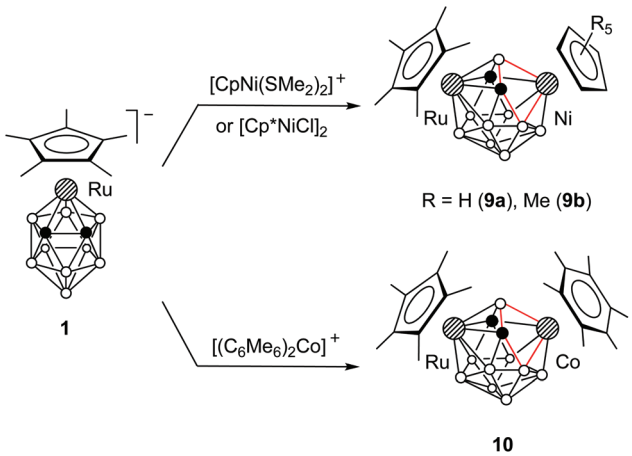

Scheme 7

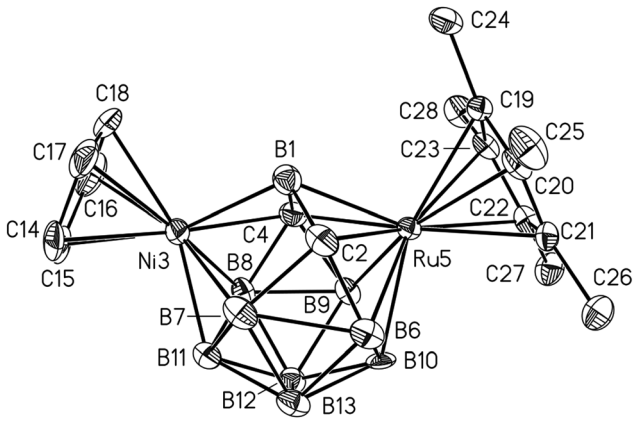

Fig. 2 The molecular structure of **9a** in 50% thermal ellipsoids. The second independent molecule and the hydrogen atoms are omitted for clarity. Selected interatomic distances (Å): Ru5–C2 2.116(5), Ru5–C4 2.199(5), Ru5–B1 2.158(6), Ru5–B6 2.225(5), Ru5–B9 2.179(5), Ru5–B10 2.238(5), Ni3···C2 2.967(5), Ni3–C4 2.081(5), Ni3–B1 2.106(6), Ni3–B7 2.302(6), Ni3–B8 2.027(6), Ni3–B11 2.074(6), B1–C2 1.542(7), B1–C4 1.674(7), Ru5···Cp* 1.861, Ni3···Cp 1.737, Ru5···Ni3 3.768(1).

(Ni3···C2 2.967, Ni3–C4 2.081 Å) and the quadrilateral open face Ni3–B1–C2–B7. In addition, the Ru5–B1 distance in **9a** (2.156 Å) is notably longer than that in **5** (2.050 Å).

Despite the asymmetry in the crystal, the ^1H and $^{11}B\{^1H\}$ NMR spectra of **9a,b** and **10** correspond to the C_s-symmetrical structure, indicating the rapid interconversion of two enantiomeric forms (Scheme 8). Apparently, the crystal structure represents a "frozen-out" extreme point of this process. We could

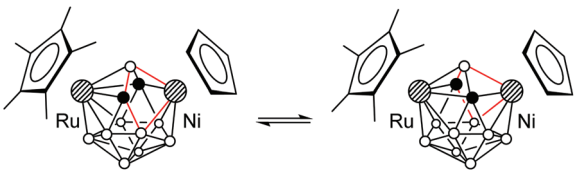

Scheme 8

not detect the unsymmetrical structure in solution by $^{11}B\{^1H\}$ NMR even at −80 °C. This means that the activation energy of this process is less than 10 kcal mol^{-1}, which is typical of 13-vertex metallacarboranes.[17] Indeed, the barrier for the unsubstituted analogue $CpRuC_2B_9H_{11}NiCp$ was calculated to be 5.1 kcal mol^{-1} (*vide infra*). It should also be noted that in contrast to **2a–d**, **5**, **7a**,**b**, and **8**, the NMR signal of the bridging B1 atom in **9a**,**b** and **10** is observed in the ordinary region at about 0 ppm. The ^1H NMR singlet of cage CH groups is found at δ = 3.88 (**9a**), 3.28 (**9b**) and 2.84 (**10**) ppm.

Electrochemical studies

The electrochemical behaviour of compounds **1**, **2b**,**d**, **5**, **6**, **9a**, **b** and **10** was studied by means of cyclic voltammetry. Their electrode potentials along with the potentials of some related complexes are compiled in Table 1.

Anion **1** undergoes a coulometrically measured one-electron oxidation which displays the features of chemical reversibility in the cyclic voltammetric time scale (Fig. 3). In fact, analysis of the cyclic voltammetric responses with scan rates varying from 0.02 V s^{-1} to 2.00 V s^{-1} shows that: (i) the current ratio i_{pc}/i_{pa} is constantly equal to 1; (ii) the current function $i_{pa}\cdot\nu^{-1/2}$ remains substantially constant; (iii) the peak-to-peak separation ranges from 60 mV to 70 mV. In the longer times of the exhaustive Ru^{II}/Ru^{III} oxidation some decomposition of the oxidised products occurs so that the complementary cyclic voltammetric response of the final deep-yellow solution is almost halved with respect to the pale-yellow original solution. It should be noted that the oxidation of the neutral analogue **6** occurs at notably higher potential values (due to both electrostatic and inductive effects) and the corresponding Ru^{III} derivative is unstable even in the short times of cyclic voltammetry (representatively, the current ratio is 0.5 at 0.05 V s^{-1} and increases to 0.8 at 2.00 V s^{-1}). Both **1** and **6** exhibit second irreversible oxidation (not shown in Fig. 3), which can be tentatively assigned to the Ru^{III}/Ru^{IV} process.

The diruthenacarborane **2b** undergoes two separate reductions both having the features of chemical reversibility

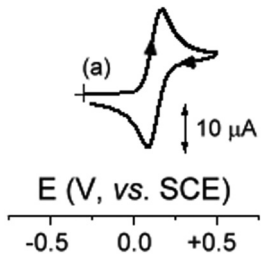

Fig. 3 Voltammetric responses recorded at a platinum electrode of 1.2 × 10^{-3} mol dm^{-3} solution of **1** in CH_2Cl_2 with the $[NBu_4][PF_6]$ (0.2 mol dm^{-3}) supporting electrolyte.

(Fig. 4). Even though controlled potential coulometry of the first process tended to consume more than one-electron/molecule, periodic cyclic voltammetric tests proved that the excess of electrons was simply due to the partial reoxidation of the reduced species probably triggered by traces of air (a drawback which is rather common in controlled potential electrolysis at rather negative potential values).

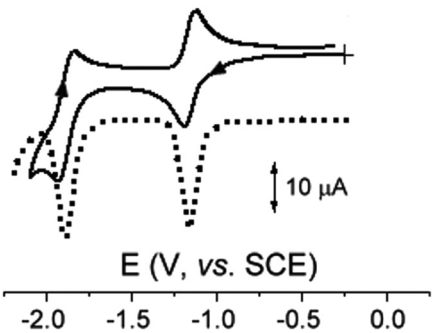

Fig. 4 Voltammetric responses recorded at a platinum electrode of 0.9 × 10^{-3} mol dm^{-3} solution of **2b** in CH_2Cl_2 with the $[NBu_4][PF_6]$ (0.2 mol dm^{-3}) supporting electrolyte. (—) Cyclic voltammetry at a scan rate of 0.2 V s^{-1}; (···) Osteryoung square wave voltammetry at a scan rate of 0.1 V s^{-1}.

Table 1 Formal electrode potentials (V, *vs.* SCE) and peak-to-peak separations (mV) for the redox changes exhibited by the present dimetallacarboranes and related species in CH_2Cl_2 solution

	Oxidations				Reductions			
Complex	$E^{\circ\prime}_{1st}$	ΔE_p [a]	$E^{\circ\prime}_{2nd}$	ΔE_p [a]	$E^{\circ\prime}_{1st}$	ΔE_p [a]	$E^{\circ\prime}_{2nd}$	ΔE_p [a]
1	+0.13	74	+0.96[a,b]	—	—	—	—	—
6	+0.70	64	+1.43[b,c]	—	—	—	—	—
2b	+1.19[b,c,d]	—	—	—	−1.15	64	−1.89	74
2d	+1.29[b,c,d]	—	—	—	−1.14	66	−1.90	110
$Cp_2Fe_2C_2B_9H_{11}$	+1.36[b,e]	—	—	—	−0.59[e]	—	—	—
5	+1.3[h]	—	—	—	−0.93	60	−1.79	60
9a	+1.10	71	+1.60[b,c,d]	—	−0.84	76	−1.88	106
9b	+0.87	64	+1.32[f]	92[f]	−1.13	70	−2.08[g]	—
10	+0.43	62	+1.33	100[i]	−1.38	60	—	—
Cp_2Fe	+0.39	68	—	—	—	—	—	—

[a] Measured at 0.2 V s^{-1}. [b] Peak-potential value for irreversible processes. [c] Measured at 1.00 V s^{-1}. [d] Multielectron process. [e] In MeCN solution, see ref. 19. [f] Measured at 2.00 V s^{-1}. [g] From DPV. [h] Ill resolved, see the text. [i] Measured at 10.24 V s^{-1}.

These sequential reductions can be formally attributed to the stepwise sequence $Ru^{II}Ru^{II}/Ru^{II}Ru^{I}/Ru^{I}Ru^{I}$ (the real reduction process involves not only the metals but rather the whole metallacarborane framework). Given the large separation of the two cathodic steps ($\Delta E^{o\prime}$ = 0.74 V), it is speculated that the electrogenerated monoanion $[\mathbf{2b}]^-$ should belong to the completely delocalised mixed-valent species (K_{com} = 3.2 × 10^{12}).[18] An irreversible oxidation of **2b** is present at very positive potential values. A substantially similar behaviour is exhibited by the permethylated analogue **2d**. For the related diferracarborane $Cp_2Fe_2C_2B_9H_{11}$ a single reversible one-electron reduction and an irreversible oxidation were described in MeCN solution.[19]

Similar to compounds **2b**,**d** heteronuclear dimetallacarborane **5** gives rise to two well separated reductions, and an irreversible oxidation process substantially combined with the solvent discharge (Fig. 5).

Let us now move to the nickel–ruthenium complexes **9a**,**b** that obey Wade's rules. As illustrated in Fig. 6a, which refers to **9a**, they undergo two chemically reversible one-electron reductions and a first chemically reversible oxidation, followed by a second oxidation which is accompanied by relatively fast chemical complications. In fact, as shown in Fig. 6(b and c), which refers to **9b**, at high scan rates the chemical complication is overcome, and also the second oxidation shows the features of chemical reversibility. Comparison of the related diruthenium and nickel–ruthenium species (in particular **2b** and **9b**) seems to support the assignment of the first oxidation and the second reduction as Ni-centred.

Finally, compound **10** (Fig. 7) also affords two well separated oxidations (the second of which, due to chemical complications, is well resolved only at high scan rates) and apparently a single reduction (even if it seems likely that the second reduction, because of the cathodic shift of the reduction process, might be obscured by the solvent discharge).

Upon exhaustive one-electron oxidation, the original red solution of **10** (λ_{max} = 477 nm) affords the quite stable green solution of $[\mathbf{10}]^+$ (λ_{max} = 690 nm). Fig. 8 shows the UV-vis spectrophotometric pattern recorded upon stepwise oxidation. The appearance of the isosbestic point following the $\mathbf{10}/[\mathbf{10}]^+$

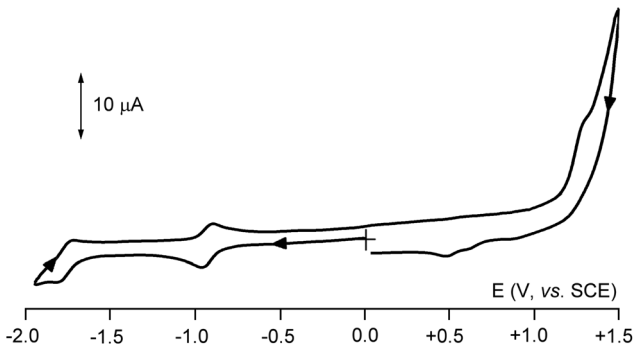

Fig. 5 Cyclic voltammogram recorded at a platinum electrode in CH_2Cl_2 solutions of **5** (1.0 × 10^{-3} mol dm^{-3}). $[NBu_4][PF_6]$ (0.2 mol dm^{-3}) supporting electrolyte. Scan rate 0.2 V s^{-1}.

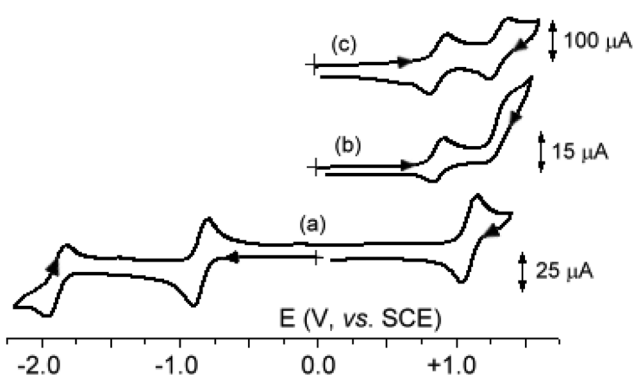

Fig. 6 Cyclic voltammograms recorded at a platinum electrode in CH_2Cl_2 solutions of: (a) **9a** (0.8 × 10^{-3} mol dm^{-3}); (b, c) **9b** (0.9 × 10^{-3} mol dm^{-3}). $[NBu_4][PF_6]$ (0.2 mol dm^{-3}) supporting electrolyte. Scan rates: (a) 2.0 V s^{-1}; (b) 0.2 V s^{-1}; (c) 10.24 V s^{-1}.

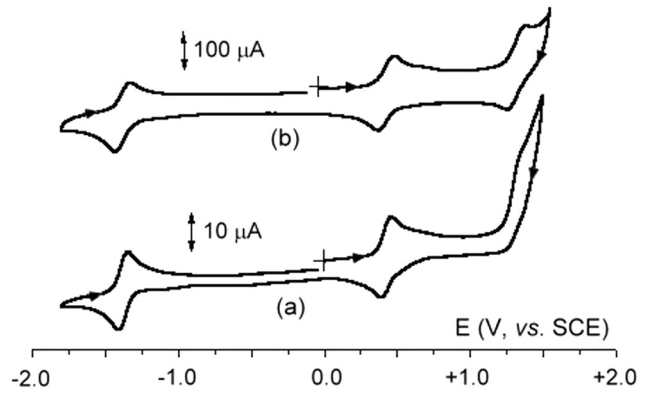

Fig. 7 Cyclic voltammograms recorded at a platinum electrode in CH_2Cl_2 solutions of **10** (0.8 × 10^{-3} mol dm^{-3}). $[NBu_4][PF_6]$ (0.2 mol dm^{-3}) supporting electrolyte. Scan rates: (a) 0.2 V s^{-1}; (b) 10.24 V s^{-1}.

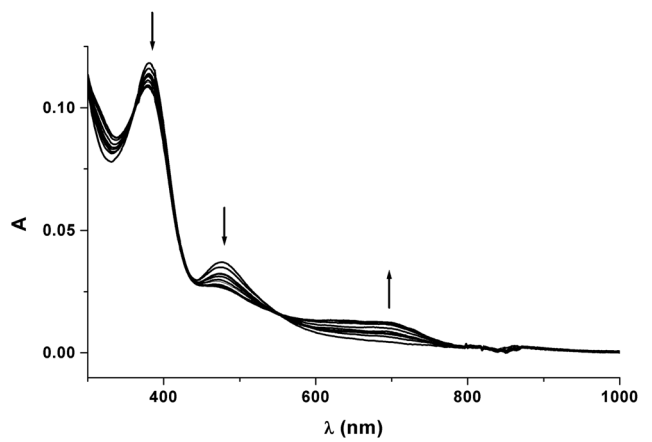

Fig. 8 Spectral changes recorded in an OTTLE cell upon progressive oxidation of **10**. CH_2Cl_2 solution. $[NBu_4][PF_6]$ (0.2 mol dm^{-3}) supporting electrolyte.

passage (λ = 551 nm) confirms the chemical reversibility of this oxidation process.

Chemical reduction of 2b

In agreement with the electrochemical data that **2b** undergoes two subsequent reversible reductions, we were able to reduce it chemically. The reaction of **2b** with one equivalent of sodium naphthalenide in THF-d_8 gives a dark-violet paramagnetic solution of $[\mathbf{2b}]^-$ and the addition of the second equivalent of $NaC_{10}H_8$ produces a dark-red diamagnetic solution of $[\mathbf{2b}]^{2-}$. The addition of acid to this solution or exposing it to air regenerates the initial compound **2b**, confirming the reversibility of the process. The $^{11}B\{^1H\}$ NMR spectrum of $[\mathbf{2b}]^{2-}$ displays 3 singlets in a 2 : 4 : 2 ratio between −5 and −20 ppm. Presumably, the signal of the bridging B1 atom is too broad and difficult to observe because of the fluxional process. The ^1H NMR spectrum of $[\mathbf{2b}]^{2-}$ shows only the Cp* signal at 1.87 ppm; the CH-cage signals are probably masked by the residual signals of THF (multiplets at 1.43 and 3.75 ppm). It should be noted that there are no signals in the high-field region, which are characteristic of compounds **2a–c**. Overall, the spectral data suggest that the dianion $[\mathbf{2b}]^{2-}$ has a structure similar to that of **9b**. Unfortunately, numerous attempts to grow up crystals of $[\mathbf{2b}]^{2-}$ for X-ray diffraction study were unsuccessful.

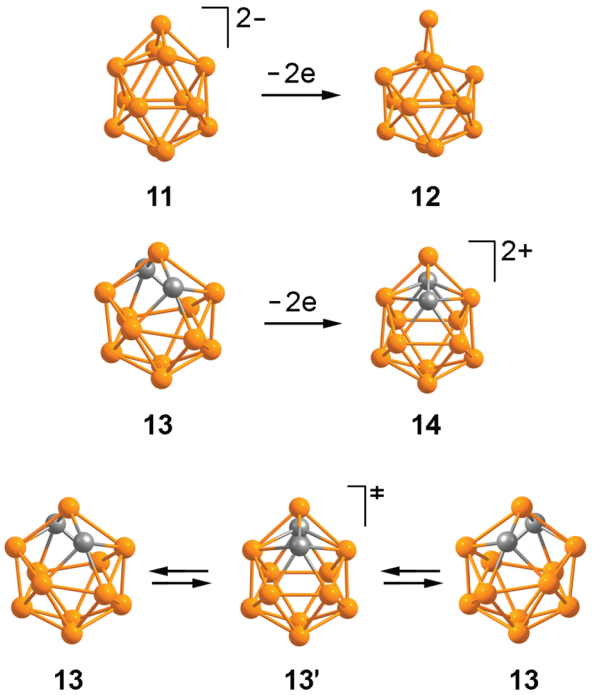

Fig. 9 The optimized structures of 13-vertex boranes and carboranes. All hydrogen atoms are omitted for clarity.

Theoretical aspects

One of the most interesting features of the dimetallacarboranes obtained is the formal violation of Wade's rules.[20] Indeed, compounds **2a–d**, **5**, **7a**,**b**, and **8** have 26 skeletal electrons (SE), while 28 are required for 13-vertex *closo*-cages.[21] At the same time, complexes **9a**,**b** and **10** have 28 SE but exhibit a significantly distorted framework. Nevertheless, all these compounds are thermally stable (at least up to 160 °C) and chemically inert. We have tried to explain this contradiction on the basis of DFT calculations.[22]

Let us first consider the hypothetical 13-vertex borane dianion $[B_{13}H_{13}]^{2-}$ (**11**) and its neutral congener $B_{13}H_{13}$ (**12**), which have 28 and 26 SE, respectively. The dianion **11** obeys Wade's rules and therefore has stable *closo*-geometry with C_{2v} symmetry (Fig. 9). Upon its oxidation to the neutral borane **12** the framework undergoes distortion with extrusion of the four-coordinated BH vertex. The resulting molecule is best described as the $\{BH\}^{2+}$ fragment coordinated with the $[B_{12}H_{12}]^{2-}$ icosahedral cage.[23,24]

The situation is different for isoelectronic carborane species $C_2B_{11}H_{13}$ (**13**) and $[C_2B_{11}H_{13}]^{2+}$ (**14**).[25] Geometry optimization of the 28 SE cluster **13** converges to the C_2-symmetrical structure with two quadrilateral open faces. The structural difference between $[B_{13}H_{13}]^{2-}$ and isoelectronic $C_2B_{11}H_{13}$ can be explained by the smaller covalent radius of carbon *vs.* boron (0.76 *vs.* 0.84).[26] Upon oxidation to **14** the carborane framework shrinks and restores the C_{2v}-symmetrical *closo*-structure. In principle, one could expect dication **14** to undergo the extrusion of the BH vertex similar to that of isoelectronic **12**. However, this would lead to the formation of C–C connectivity, which is unfavorable because of the electrostatic repulsion.[27] Thus, the introduction of two carbon atoms instead of borons dramatically changes the geometric and electronic preferences of the 13-vertex framework.

Interestingly, the C_{2v}-symmetrical *closo*-structure of $C_2B_{11}H_{13}$, **13′**, is less stable than **13** by 8.4 kcal mol^{-1} and corresponds to the transition state for the interconversion of two enantiomeric forms of **13**. Close energies of **13** and **13′** suggest that $C_2B_{11}H_{13}$ should be fluxional in solution.

The calculated structures of the 13-vertex dimetallacarboranes are generally similar to those of isoelectronic carboranes. Thus, the optimization of 26 SE diruthenacarborane **2c** gives the expected C_{2v}-symmetrical *closo*-geometry, which correlates with the experimental structure of **2b** (Fig. 10). The 28 SE nickelaruthenacarborane $CpNi(C_2B_9H_{11})RuCp$ can adopt two structures **15** and **15′** with C_1 and C_s symmetry, respectively (similar to **13** and **13′**). The unsymmetrical structure **15** was found to be only 5.1 kcal mol^{-1} more stable than **15′**. Such a small energy difference explains the distorted structure of **9a** in the crystal and its fluxionality in solution (*vide supra*).

The mechanism of electrophilic insertion has been investigated computationally for the model reaction between $[CpRuC_2B_9H_{11}]^-$ and $[CpRu]^+$ giving **2c** (Fig. 11). The initial interaction of these ions leads to the *exo–closo* intermediate **16**.[28] Interestingly, **16** has a substantially opened framework with well separated carbon atoms (C···C 2.476 Å), which presumably facilitate further rearrangement. A similar opening upon *exo*-coordination has been recently observed for carborane-Os3 clusters.[29] The insertion proceeds *via* a transition

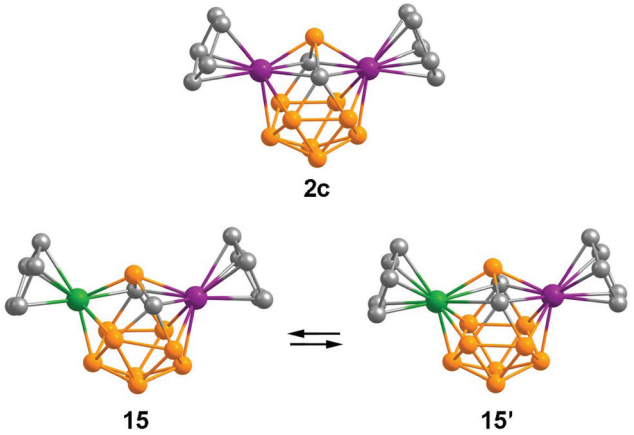

Fig. 10 The optimized structures of 13-vertex dimetallacarboranes. All hydrogen atoms are omitted for clarity.

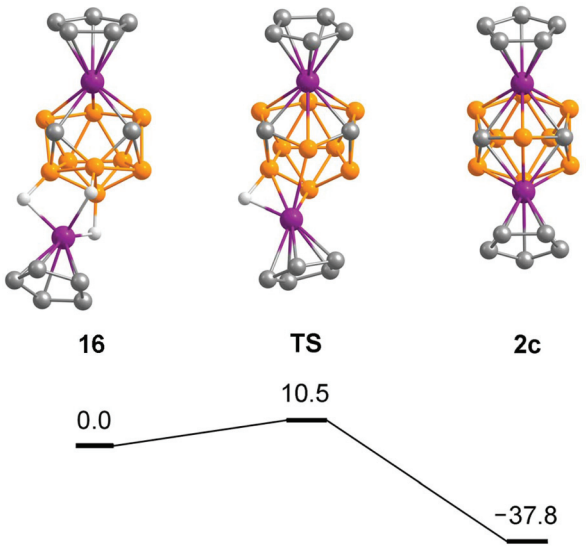

Fig. 11 Calculated mechanism for the insertion of $[CpRu]^+$ into $[CpRuC_2B_9H_{11}]^-$. All hydrogen atoms except those participating in Ru–H–B bonds are omitted for clarity. The energies are given relative to **16** in kcal mol^{-1}.

state (TS) with a low activation barrier (10.5 kcal mol^{-1}) correlating with the fast reaction in experiment. The final formation of diruthenacarborane **2c** is 37.8 kcal mol^{-1} favorable.

Conclusion

Reaction of electrophilic insertion of $[M(ring)]^+$ species into 12-vertex *closo*-ruthenacarboranes was studied. The insertion of 12-electron species gives 13-vertex 26 SE *closo*-dimetallacarboranes which formally violate Wade's rules. The insertion of 14-electron species gives 13-vertex 28 SE dimetallacarboranes which are distorted in the crystal and fluxional in solution. According to cyclic voltammetry, 26 SE dimetallacarboranes can undergo two sequential one-electron reduction, while 28 SE compounds exhibit double oxidation. The DFT calculations suggest that the violation of Wade's rules observed for the 13-vertex dimetallacarboranes is mainly because of the repulsion of the cage carbon atoms and their small covalent radii.

Conflicts of interest

There are no conflicts to declare.

Acknowledgements

We thank the Russian Science Foundation (grant # 17-73-30036) for financial support. The X-ray diffraction data were obtained using the equipment of the Center for Molecular Composition Studies of INEOS RAS.

References

1 (*a*) R. N. Grimes, *Carboranes*, 3rd edn, Academic Press, New York, 2016; (*b*) M. F. Hawthorne and G. B. Dunks, *Science*, 1972, **178**, 462.
2 (*a*) E. S. Stoyanov, I. V. Stoyanova and C. A. Reed, *J. Am. Chem. Soc.*, 2011, **133**, 8452 and references therein; (*b*) C. A. Reed, *Acc. Chem. Res.*, 2010, **43**, 121; (*c*) I. Krossing and I. Raabe, *Angew. Chem., Int. Ed.*, 2004, **43**, 2066.
3 (*a*) E. A. Qian, A. I. Wixtrom, J. C. Axtell, A. Saebi, P. Rehak, Y. Han, E. H. Moully, D. Mosallaei, S. Chow, M. Messina, J.-Y. Wang, A. T. Royappa, A. L. Rheingold, H. D. Maynard, P. Kral and A. M. Spokoyny, *Nat. Chem.*, 2017, **9**, 333; (*b*) M. S. Messina, J. C. Axtell, Y. Wang, P. Chong, A. I. Wixtrom, K. O. Kirlikovali, B. M. Upton, B. M. Hunter, O. S. Shafaat, S. I. Khan, J. R. Winkler, H. B. Gray, A. N. Alexandrova, H. D. Maynard and A. M. Spokoyny, *J. Am. Chem. Soc.*, 2016, **138**, 6952; (*c*) L. Ma, J. Hamdi, F. Wong and M. F. Hawthorne, *Inorg. Chem.*, 2006, **45**, 278; (*d*) T. Li, S. S. Jalisatgi, M. J. Bayer, A. Maderna, S. I. Khan and M. F. Hawthorne, *J. Am. Chem. Soc.*, 2005, **127**, 17832; (*e*) O. K. Farha, R. L. Julius, M. W. Lee, R. E. Huertas, C. B. Knobler and M. F. Hawthorne, *J. Am. Chem. Soc.*, 2005, **127**, 18243.
4 (*a*) R. Núñez, M. Tarrés, A. Ferrer-Ugalde, F. Fabrizi de Biani and F. Teixidor, *Chem. Rev.*, 2016, **116**, 14307; (*b*) C. E. Housecroft, *J. Organomet. Chem.*, 2015, **798**, 218; (*c*) J. Guo, D. Liu, J. Zhang, J. Zhang, Q. Miao and Z. Xie, *Chem. Commun.*, 2015, **51**, 12004; (*d*) O. K. Farha, A. M. Spokoyny, K. L. Mulfort, M. F. Hawthorne, C. A. Mirkin and J. T. Hupp, *J. Am. Chem. Soc.*, 2007, **129**, 12680; (*e*) K. Vyakaranam, S. Körbe and J. Michl, *J. Am. Chem. Soc.*, 2006, **128**, 5680.
5 (*a*) O. Tutusaus, C. Viñas, R. Núñez, F. Teixidor, A. Demonceau, S. Delfosse, A. F. Noels, I. Mata and E. Molins, *J. Am. Chem. Soc.*, 2003, **125**, 11830; (*b*) Z. Yinghuai, L. C. Nong, L. C. Zhao, E. Widjaja,

C. S. Hwei, W. Cun, J. Tan, M. V. Meurs, N. S. Hosmane and J. A. Maguire, *Organometallics*, 2009, **28**, 60.

6 For some recent papers see: (*a*) A. Robertson, N. Beattie, G. Scott, W. Man, J. Jones, S. A. Macgregor, G. M. Rosair and A. J. Welch, *Angew. Chem., Int. Ed.*, 2016, **55**, 8706; (*b*) W. Man, D. Ellis, G. M. Rosair and A. J. Welch, *Angew. Chem., Int. Ed.*, 2016, **55**, 4596; (*c*) A. McAnaw, M. E. Lopez, D. Ellis, G. M. Rosair and A. J. Welch, *Dalton Trans.*, 2014, **43**, 5095; (*d*) K. J. Dalby, D. Ellis, S. Erhardt, R. D. McIntosh, S. A. Macgregor, K. Rae, G. M. Rosair, V. Settels, A. J. Welch, B. E. Hodson, T. D. McGrath and F. G. A. Stone, *J. Am. Chem. Soc.*, 2007, **129**, 3302; (*e*) J. Zhang, L. Deng, H.-S. Chan and Z. Xie, *J. Am. Chem. Soc.*, 2007, **129**, 18; (*f*) L. Deng, J. Zhang, H.-S. Chan and Z. Xie, *Angew. Chem., Int. Ed.*, 2006, **45**, 4309; (*g*) R. D. McIntosh, D. Ellis, G. M. Rosair and A. J. Welch, *Angew. Chem., Int. Ed.*, 2006, **45**, 4313; (*h*) L. Deng, H.-S. Chan and Z. Xie, *J. Am. Chem. Soc.*, 2006, **128**, 5219.

7 For reviews see: (*a*) J. Zhang and Z. Xie, *Acc. Chem. Res.*, 2014, **47**, 1623; (*b*) L. Deng and Z. Xie, *Coord. Chem. Rev.*, 2007, **251**, 2452.

8 This method was pioneered by Hawthorne *et al.* See: (*a*) D. F. Dustin, G. B. Dunks and M. F. Hawthorne, *J. Am. Chem. Soc.*, 1973, **95**, 1109; (*b*) W. J. Evans and M. F. Hawthorne, *Inorg. Chem.*, 1974, **13**, 869.

9 (*a*) V. R. Miller, L. G. Sneddon, D. C. Beer and R. N. Grimes, *J. Am. Chem. Soc.*, 1974, **96**, 3090; (*b*) W. M. Maxwell, E. Sinn and R. N. Grimes, *J. Am. Chem. Soc.*, 1976, **98**, 3490; (*c*) M. Green, J. L. Spencer and F. G. A. Stone, *J. Chem. Soc., Dalton Trans.*, 1979, 1679 and references therein; (*d*) M. P. Garcia, M. Green, F. G. A. Stone, R. G. Somerville, A. J. Welch, C. E. Briant, D. N. Cox and D. M. P. Mingos, *J. Chem. Soc., Dalton Trans.*, 1985, 2343; (*e*) X. L. R. Fontaine, H. Fowkes, N. N. Greenwood, J. D. Kennedy and M. Thornton-Pett, *J. Chem. Soc., Dalton Trans.*, 1987, 2417; (*f*) M. Bown, X. L. R. Fontaine, N. N. Greenwood, J. D. Kennedy and M. Thornton-Pett, *J. Chem. Soc., Dalton Trans.*, 1988, 925 and references therein; (*g*) A. Fessenbecker, M. Stephan, R. N. Grimes, H. Pritzkow, U. Zenneck and W. Siebert, *J. Am. Chem. Soc.*, 1991, **113**, 3061.

10 For preliminary communication see: A. R. Kudinov, D. S. Perekalin, S. S. Rynin, K. A. Lyssenko, G. V. Grintselev-Knyazev and P. V. Petrovskii, *Angew. Chem., Int. Ed.*, 2002, **41**, 4112.

11 A. R. Kudinov, M. I. Rybinskaya, Yu. T. Struchkov, A. I. Yanovskii and P. V. Petrovskii, *J. Organomet. Chem.*, 1987, **336**, 187.

12 Similar species were obtained in the reactions of *closo*-carborane and metallacarborane anions with BF_3 in THF. See for example: A. A. Semioshkin, I. B. Sivaev and V. I. Bregadze, *Dalton Trans.*, 2008, 977.

13 (*a*) M. V. Butovskii, U. Englert, A. A. Fil'chikov, G. E. Herberich, U. Koelle and A. R. Kudinov, *Eur. J. Inorg. Chem.*, 2002, 2656; (*b*) E. V. Mutseneck, D. A. Loginov, D. S. Perekalin, Z. A. Starikova, D. G. Golovanov, P. V. Petrovskii, P. Zanello, M. Corsini, F. Laschi and A. R. Kudinov, *Organometallics*, 2004, **23**, 5944; (*c*) A. R. Kudinov, E. V. Mutseneck and D. A. Loginov, *Coord. Chem. Rev.*, 2004, **248**, 571.

14 Diruthenacarboranes **7a,b** were initially assigned the triple-decker structures based on ^{1}H and ^{11}B NMR. See: A. R. Kudinov, P. V. Petrovskii, V. I. Meshcheryakov and M. I. Rybinskaya, *Russ. Chem. Bull.*, 1999, **48**, 1356.

15 Down-field signals are characteristic of low-coordinated boron atoms, especially close to the metals. See: R. S. Coldicott, J. D. Kennedy and M. Thornton-Pett, *J. Chem. Soc., Dalton Trans.*, 1996, 3819.

16 A. R. Kudinov, M. I. Rybinskaya, D. S. Perekalin, V. I. Meshcheryakov, Yu. A. Zhuravlev, P. V. Petrovskii, A. A. Korlykov, D. G. Golovanov and K. A. Lyssenko, *Russ. Chem. Bull.*, 2004, **53**, 1958.

17 (*a*) N. M. M. Wilson, D. Ellis, A. S. F. Boyd, B. T. Giles, S. A. Macgregor, G. M. Rosair and A. J. Welch, *J. Chem. Soc., Chem. Commun.*, 2002, 464; (*b*) M. A. Laguna, D. Ellis, G. M. Rosair and A. J. Welch, *Inorg. Chem. Acta*, 2003, **347**, 161; (*c*) A. Burke, D. Ellis, D. Ferrer, D. L. Ormsby, G. M. Rosair and A. J. Welch, *Dalton Trans.*, 2005, 1716; (*d*) R. McIntosh, D. Ellis, J. Gil-Lostes, K. J. Dalby, G. M. Rosair and A. J. Welch, *Dalton Trans.*, 2005, 1842.

18 P. Zanello, *Inorganic Electrochemistry. Theory, Practice and Application*, RSC, United Kingdom, 2003.

19 C. G. Salentine and M. F. Hawthorne, *Inorg. Chem.*, 1978, **17**, 1498.

20 (*a*) A. J. Welch, *Chem. Commun.*, 2013, **49**, 3615; (*b*) E. D. Jemmis, M. M. Balakrishnarajan and P. D. Pancharatna, *J. Am. Chem. Soc.*, 2001, **123**, 4313.

21 Several isomers of the 13-vertex $Cp_2Fe_2C_3B_8H_{11}$ are also stable with 1 electron less than required by Wade's rules: B. Grüner, B. Štibr, R. Kivekäs, R. Sillanpää, P. Stopka, F. Teixidor and C. Viñas, *Chem. – Eur. J.*, 2003, **9**, 6115.

22 Such violation of Wade's rules was previously explained by the non-degenerate HOMO of $[B_{13}H_{13}]^{2-}$, which can remain empty without significant distortion of the framework. See: M. E. Lopez, M. J. Edie, D. Ellis, A. Horneber, S. A. Macgregor, G. M. Rosair and A. J. Welch, *Chem. Commun.*, 2007, 2243.

23 Our results correlate well with the results of B3LYP/6-31G* calculations: M. L. McKee, Z.-X. Wang and P. v. R. Schleyer, *J. Am. Chem. Soc.*, 2000, **122**, 4781.

24 According to calculations further distortion of the structure of $B_{13}H_{13}$ can proceed with tilting of the exocyclic BH vertex. However, this is not important for the current discussion.

25 For recent calculations of supraicosahedral carboranes $C_2B_{n-2}H_n$ see: J. Zhang, Z. Lin and Z. Xie, *Organometallics*, 2015, **34**, 5576.

26 B. Cordero, V. Gómez, A. E. Platero-Prats, M. Revés, J. Echeverría, E. Cremades, F. Barragán and S. Alvarez, *Dalton Trans.*, 2008, 2832.

27 It has been confirmed both computationally and experimentally that C–C connectivity in the cluster decreases the thermodynamic stability of carboranes and metallacar-

boranes: (*a*) J. M. Oliva, N. L. Allan, P. V. R. Schleyer, C. Viñas and F. Teixidor, *J. Am. Chem. Soc.*, 2005, **127**, 13538; (*b*) D. S. Perekalin and A. R. Kudinov, *Russ. Chem. Bull.*, 2005, **54**, 1603; (*c*) F. A. Kiani and M. Hofmann, *Dalton Trans.*, 2006, 686.

28 *Exo–closo*-metallacarboranes are well-known and structurally characterized. In some cases they are suggested as intermediates in insertion reactions. See for example: (*a*) I. V. Pisareva, V. E. Konoplev, P. V. Petrovskii, E. V. Vorontsov, F. M. Dolgushin, A. I. Yanovsky and I. T. Chizhevsky, *Inorg. Chem.*, 2004, **43**, 6228; (*b*) S. Du, J. C. Jeffery, J. A. Kautz, X. L. Lu, T. D. McGrath, T. A. Miller, T. Riis-Johannessen and F. G. A. Stone, *Inorg. Chem.*, 2005, **44**, 2815.

29 R. D. Adams, J. Kiprotich, D. V. Peryshkov and Y. O. Wong, *Chem. – Eur. J.*, 2016, **22**, 6501.